

Chapter 14

DC Grid Interconnection for Conversion Losses and Cost Optimization

R. K. Chauhan, B. S. Rajpurohit, S. N. Singh
and F. M. Gonzalez-Longatt

Abstract The rapid increment of DC compatible appliances in the buildings, emerge the photovoltaic energy as the fastest growing source of renewable energy and expected to see continued strong growth in the immediate future. The photovoltaic power is, therefore, required to be provided with a certain reliability of supply and a certain level of stability. Motivated by the above issues, many grid operators have to develop DC micro-grids, which treat photovoltaic power generation in a special manner. The interconnection of different voltage rating distributed generation, storage and the load to the DC micro-grid requires large number of converters, which will increase the conversion power losses and the installation cost. Different types of Low Voltage Direct Current (LVDC) grid and their topologies are helpful in understanding the interconnection of distributed generation with consumers end. The connections of LVDC distribution system is discussed in this chapter. Optimization of LVDC grid voltage may reduce the conversion stage and the power loss in DC feeders. A multi-objective technique is discussed, in this chapter, to design a minimum power loss and low cost DC micro-grid.

R. K. Chauhan (✉) · B. S. Rajpurohit
School of Computing and Electrical Engineering, Indian Institute of Technology Mandi,
Mandi, Himachal Pradesh 175001, India
e-mail: rkchr_iitm@yahoo.com

B. S. Rajpurohit
e-mail: bsr@iitmandi.ac.in

S. N. Singh
Department of Electrical Engineering, Indian Institute of Technology Kanpur, Kanpur,
Uttar Pradesh 208016, India
e-mail: snsingh@iitk.ac.in

F. M. Gonzalez-Longatt
Coventry University, Faculty of Engineering and Computing EC3-32, Priory Street,
Coventry CV1 5FB, UK
e-mail: francisco.gonzalez-longatt@coventry.ac.uk

Keywords DC-DC converter · DC load · Hybrid electric vehicle · LVDC grid · Photovoltaic

14.1 Introduction

In the last decade, micro-grids have become a more attractive option for rural electrification compared with the extension of electrical transmission infrastructure to connect rural areas to the centralized grid. DC power transmission and its significance have been explained in detail [1]. According to world energy outlook 2011, around 70 % rural area will be connected to a micro-grid or standalone off grid solution while only 30 % rural areas may be connected to the main grid [2]. Rapid increment in DC appliances and the integration of Distributed Generation (DG), Hybrid Electrical Vehicles (HEV) leads to change in the structure of AC power systems as well as the direction of power flow from a single direction to bidirectional in the distribution systems [3, 4]. In [5], a review has been given about the demand and economics of Renewable Energy Resources (RESs). The DC power of RESs such as Photovoltaic (PV), and the fuel cell has to converted to AC for feeding to AC grid, while AC power have to be convert into DC power at storage and load ends, resulting in more conversion losses, and poor efficiency. For high power quality distributed resources have been used in combination with DC distribution system [6].

The consumption of DC power by the DC appliances eliminates the conversion stages required in the present AC distribution system. Moreover, the DC systems are free from inductance, capacitance effects and skin effect, resulting in a lesser voltage drop, power loss and line resistance. The DC system also requires less amount of insulation than an AC system because of lesser potential stress for same working voltage. Moreover, the multilevel voltage transformation ability of DC system promotes to interconnect the different voltage level and power rating DG sources and battery bank. It will go to increase the stability and reliability of the distribution system.

The DC load is supplied by DC power generated from load site DC sources and stored energy dramatically improves the system efficiency, reduces energy costs and environmental impact. On the other hand, the optimization of the voltage level of the DC distribution system is the most important factor for reduction in conversion losses and stages. A power-sharing method presents the control modes of micro-grid when multiple distributed generators have been connected [7]. Some literature explains the power sharing for hybrid power system [8]. Moreover, the conversion of existing AC distribution systems into the DC distribution systems is the greatest challenge for electrical engineers.

In the present scenario, Low Voltage Direct Current (LVDC) distribution systems do not have standard voltage ratings as in the case of AC distribution systems. The non-standardized voltage rating of the DC distribution systems again requires more number of DC-DC conversion stages at the load, storage and the generation ends, resulting in an increase in the conversion stages, losses and

Table 14.1 Losses based on partial AC and DC loading of power systems [16]

Loads	AC (Watt)	DC (Watt)	DC (Watt)	DC (Watt)
AC % / DC %		95 % ^a	97 % ^a	95 % ^a
100/0 ^b	412	2317	1811	1119
50/50 ^b	1679	1982	1313	583
0/100 ^b	2872	1653	1008	329

^a Represents DC–DC converter efficiency

^b Represents ratio of AC/DC loads

system cost. However, some literatures are available on the DC-DC converter and AC-DC converter for renewable energy systems [9–15]. Table 14.1 shows the conversion losses based on partial AC and DC loading of power system [16]. Three efficiencies viz. 95, 97, and 99.5 % were assigned to the DC-DC converters for their comparative study.

The I^2R loss can be represented by varying the voltages of the DC system. From this Table, the difference in loss compared to the AC become small for 95 % DC-DC converter, if 50 % of the loads are AC and 50 % of the loads are DC.

This chapter includes the topics which deals with not only the AC-DC-AC-DC, DC-AC-DC conversion stages, but also the topics related to the reduction of the DC-DC conversion stages, losses including system cost strategy in Indian environment. Moreover, the conversion of wiring such as conversion of the existing AC distribution system i.e. three-phase three-wire system, three-phase four-wire system, etc. into multi-pole DC distribution system without any change in the hardware is also discussed. The present chapter discusses the conversion losses in the DC and AC distribution systems. Different topologies have been discussed which may be helpful in reducing converter stages i.e. decreasing the conversion losses. Total cost of the DC system has been calculated and some methods for cost optimization have been explained.

14.2 Topologies of Different LVDC Grids

14.2.1 Topologies of Mini-Grid

“Mini-grid having the more expansion of serving. It is an electrical power system that having the span between two points to fulfil the requirements of more than one building” [17].

The converters and DC links are the main parts of DC distribution system. The AC-DC conversion occurs near to the Medium Voltage (MV) line in each topology. However, the points of DC-AC conversion may be at any locations. The location, where DC-AC conversion is located at consumer range, is called the wide LVDC distribution and the High Voltage Direct Current (HVDC) link may be DC-AC conversion locations [18, 19]. Figure 14.1 represents the wide LVDC

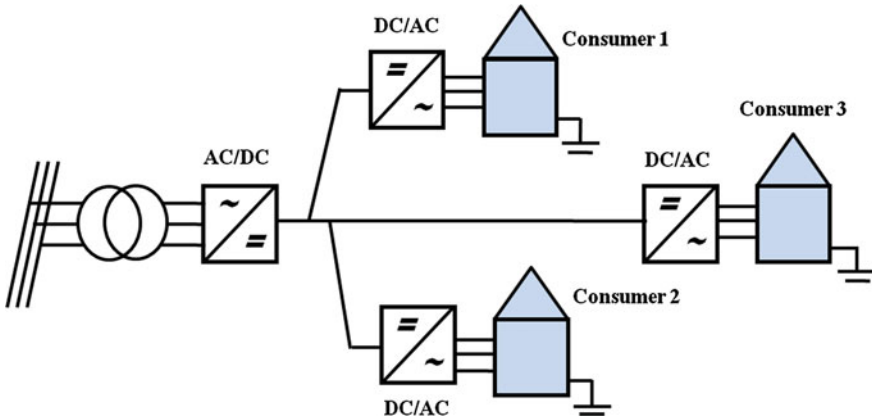


Fig. 14.1 Wide LVDC distribution system

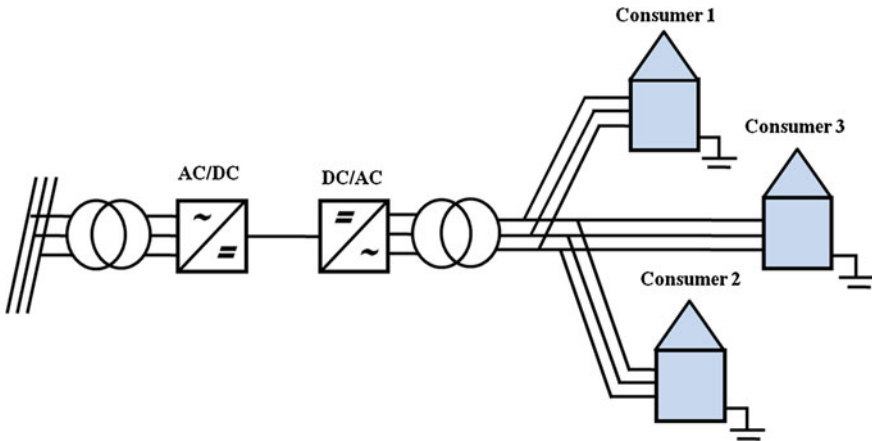


Fig. 14.2 HVDC link distribution systems

distribution system. The three-phase three-wire AC system is replaced here by single DC line [20].

In Fig. 14.2, a DC line showing a HVDC link based DC distribution system interconnects two separate AC networks. To make a suitable connection with existing AC system, DC links are connected using transformers.

14.2.2 Topologies of Micro-Grid

“A DC micro-grid is a group of many distributed energy resources which have the capability to fulfill a specified load demand by a sufficient energy continuously” [17].

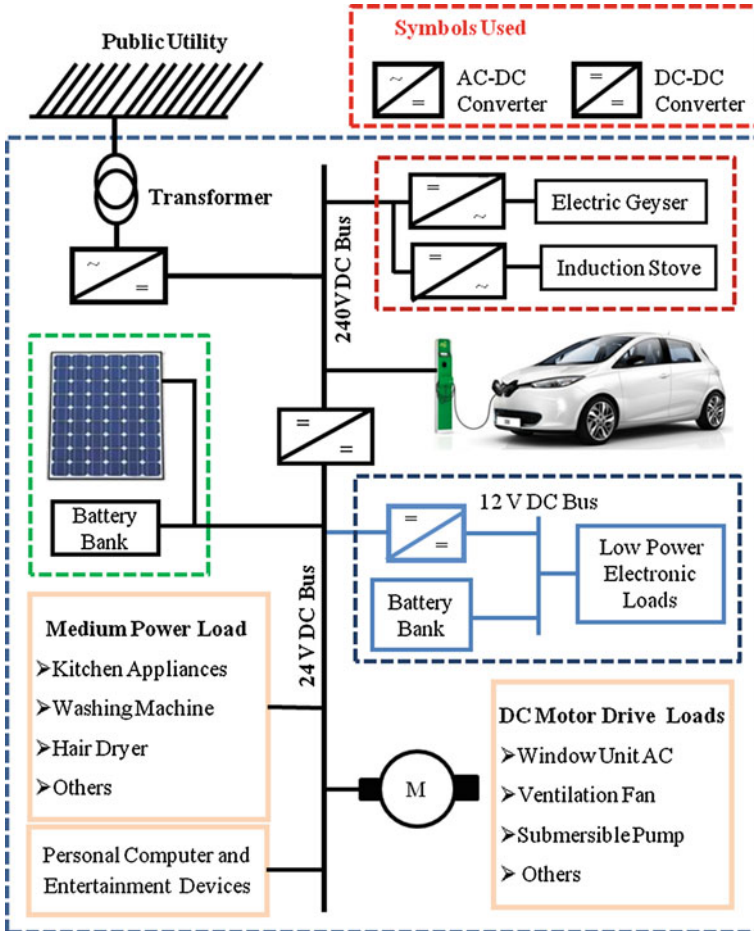


Fig. 14.3 Layout of hybrid home power system (DC Micro-Grid)

The layout of a DC micro-grid is shown in Fig. 14.3. This micro-grid structure is a combination of three 240 volt (HVDC), 24 and 12 volt (LVDC) buses to draw the three different types of loads viz. 240 volt, 24 and 12 volt loads in a same building. The power fed to the HVDC bus (240 volt DC) is supplied by external AC system via AC-DC converter while the photovoltaic plant and battery bank are connected to the LVDC bus (24 volt DC). The Buck-boost converter is used to interconnect the HVDC and LVDC buses. The HVDC bus is responsible to supply the AC compatible appliances via DC-AC converter and the hybrid car. The photovoltaic panel, battery bank and other appliances of 24 volt voltage rating has been directly connected to LVDC bus and is used to supply the power to the low power rating equipments such as DC motor drive loads, personal computer, medium power load etc. While the 12 volt LVDC bus is designed for low power

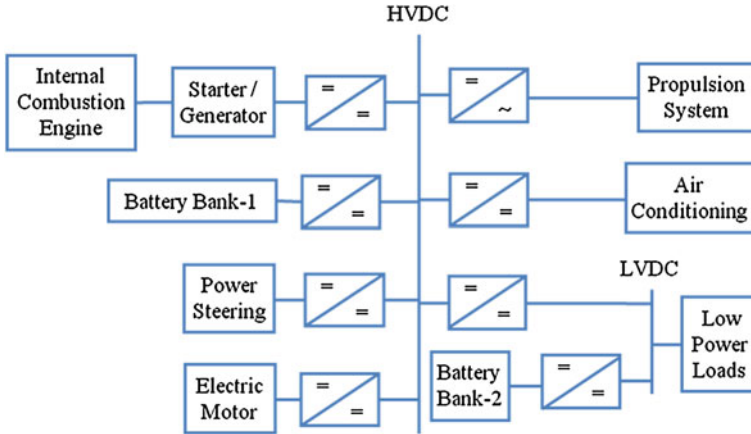


Fig. 14.4 Layout of hybrid electrical vehicle power system (Nano-Grid)

electronic appliances such as mobile. The power balancing in DC micro-grid could be achieved by the AC-DC network converter and photovoltaic, battery bank and storage DC-DC converters equipped with DC voltage regulator, which adjusts the voltage in all the buses.

14.2.3 Topologies of Hybrid Electric Vehicle (DC Nano-Grid)

“Nano-grid is an electrical power system, defined between two universal points for fulfilling the demand of a particular space in any building” [17].

Hybrid Electric Vehicle (HEV) designs is made up of a gasoline engine, a fuel tank, an electric motor, a generator, batteries and a transmission system. The electric motor, generator and batteries all work to gather on behalf of the hybrid concept. Motors not only help power the car, but can also act as generators. It means they can draw energy from the batteries, as well as return energy to the batteries. The generator itself works solely to produce electrical power, while the batteries store the energy to electric motors. Fig. 14.4 shows the layout of DC hybrid electric vehicle (nano-grid) including distributed battery bank. According to the load, the HEV power system is divided into HVDC and LVDC bus. The power fed to the HVDC bus is supplied by the generator and battery bank-1 via DC-DC converter. The HVDC bus is also connected to the propulsion system via DC-AC converter. The air conditioning, power steering, and electric motor have different operating voltage level and they are connected to HVDC bus via its own DC-DC converter. The DC-DC converters interconnect the HVDC and battery bank-2 to LVDC bus is responsible for power balancing in LVDC bus.

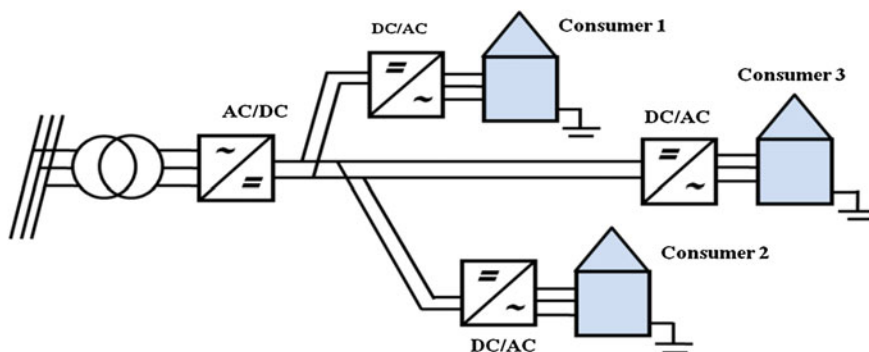


Fig. 14.5 Unipolar LVDC distribution system

14.3 LVDC System Connections

The LVDC distribution system may be categorized in two parts according to the polarities of conductor.

14.3.1 Unipolar LVDC System

The construction of a unipolar system has two conductors with neutral and positive polarity. The energy in the unipolar system is transmitted via single voltage level, by which all consumers are connected. Fig. 14.5 shows a unipolar DC system.

14.3.2 Bipolar LVDC System

Bipolar system is a combination of two series connected unipolar system. The consumers may be connected between different voltage levels as shown in Fig. 14.6. The consumer connections 1 and 2 can lead unsymmetrical loading situations between DC poles in system. The overvoltage is consequence of current superposition at neutral wire. The possible overvoltage can be restricted with cable cross-section selection and the equal load balancing. The load balancing may be achieved by placing the load between positive pole and neutral, negative pole and neutral, positive and negative poles, and positive and negative poles with neutral connection. The connections 1 and 2 are chosen to be used in studied of ± 120 volt DC bipolar system. The main lines of system contain all three conductors but at consumer end 2-wire cables connected between positive or negative pole. Therefore, the consumer supply voltage is either +120 VDC or -120 VDC [20, 21].

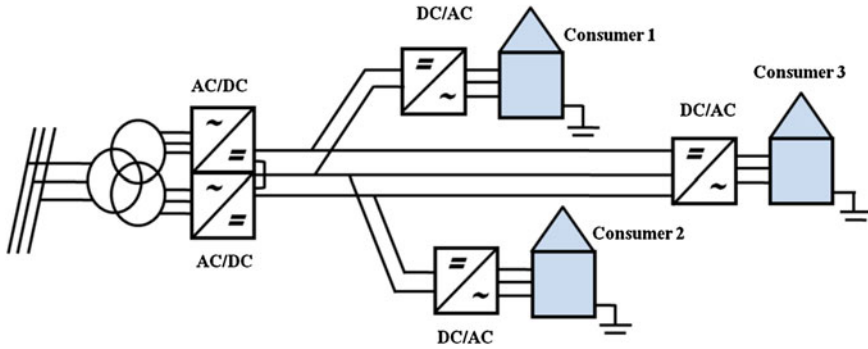


Fig. 14.6 Bipolar LVDC distribution system with different consumer connection

14.4 DC-DC Converter Efficiency

In this section, the formulation of minimum required efficiency of DC-DC converter of DC distribution system is discussed. This formulation has the ability to make the efficiency of the DC distribution system near to any AC distribution system. A step-by-step approach is used to derive the technique.

- Step1

In order to match the overall efficiency of DC system with the AC distribution system, under the constraints of same load, the total power taken in $P_{totalin}$ should be same [22]. The system total power input can be expressed as:

$$P_{totalin} = \delta P_{dli} + P_{closeses} \tag{14.1}$$

where, δ is the number of DC/DC converters distribution levels in the distribution system, $P_{closeses}$ the losses in the distribution feeders transporting power from the bulk power source to the distribution level converters.

In the DC distribution system, individual distribution level DC-DC converter power P_{dli} can be obtained by an iterative process. A seed value is required in the beginning of the iterative process. P_{dli} is considered as the seed value and can be found as:

$$P_{dli} = \frac{(\gamma \cdot P_{bulin} + P_{Closeses})}{\eta_{dl}} \tag{14.2}$$

where γ , the number of residential buildings served by one distribution level DC/DC converter, η_{dl} , the efficiency of the converter, P_{bulin} the power input in one building. It can be concluded that:

$$P_{dli} > \gamma \cdot P_{bulin} > \gamma \cdot (P_I + P_{AC} + P_{DC}) \tag{14.3}$$

Table 14.2 Description of categories with percentage loading

Category	Description	Relative Percentage
AC	Loads utilizing AC power	33.26
DC	Loads utilizing DC power	66.00
I	Loads that can use both (Independent loads)	0.74

where P_I , P_{AC} and P_{DC} represent power requirements of the three categories as listed in Table 14.2.

In the present scenario three types of load such as AC compatible, DC compatible and AC-DC compatible load can be found in the building. The relative percentage of these loads has been described in Table 14.2.

Due to power losses in the house hold converters, P_{dli} may be assumed slightly higher than the total power consumed in the loads. The iterative process solves for voltage and current values at each distribution level converter, starting from the source side. Once the far end is reached, the following equality is tested,

$$V_{cal} \times I_{cal} = P_{cal} = P_{dli_assumed} \quad (14.4)$$

where V_{cal} the calculated voltage, I_{cal} the calculated current, P_{cal} the calculated total power input to the building, $P_{dli_assumed}$ is the assumed total power input to the building.

If the equality holds, then $P_{dli_assumed}$ is the actual value of power input for the system. Otherwise, iteration is performed again with a modified value of P_{dli} . The modification depends upon the results of the previous iteration. Specifically, if

$$V_{cal} \times I_{cal} < P_{dli_assumed} \quad (14.5)$$

- Step 2

The individual building input power P_{bulin} can be expressed as:

$$P_{bulin} = P_I + \frac{(P_{AC} + P_{DC})}{\eta_{PEC}} \quad (14.6)$$

where, η_{PEC} is the Power Electronics Converter (PEC) used in appliances.

Substituting expressions of P_{bulin} and cable losses in Eq. (14.2), and choosing a suitable value for η_{dl} , the resultant can be simplified to produce the following equation.

$$P_{dli} = a \cdot \eta_{PEC}^{-2} + b \cdot \eta_{PEC}^{-1} + \rho \quad (14.7)$$

where,

$$a = \frac{R \cdot (P_{AC} + P_{DC})^2}{V_b^2} \times \frac{\gamma}{\eta_{dl}} \quad (14.8)$$

$$b = \left[(P_{AC} + P_{DC}) + \frac{2P_I \cdot (P_{AC} + P_{DC})}{V_b^2} \right] \times \frac{\gamma}{\eta_{dl}} \quad (14.9)$$

$$\rho = \left[P_I + \frac{P_I^2}{V_b^2} \times R \right] \times \frac{\gamma}{\eta_{dl}} \quad (14.10)$$

where V_b the voltage at each housing unit, R the resistance of power conductor from distribution converter to individual buildings. Equation (14.7) can be further simplified as

$$a' \cdot \eta_{PEC}^{-2} + b' \cdot \eta_{PEC}^{-1} + \lambda' = 0 \quad (14.11)$$

a' , b' are remain the same as a , b while

$$\lambda' = \left[P_I + \frac{P_I^2}{V_b^2} \times R \right] \times \frac{\gamma}{\eta_{dl}} - P_{dli} \quad (14.12)$$

14.5 Loss Calculation in DC System

14.5.1 Cable Loss

A DC system has only active power. If the load power consumption and cable type are same as AC then current and corresponding power losses in a DC system can be expressed as [23]:

$$I_{dc} = \frac{P}{V_{dc}} \quad (14.13)$$

where, I_{dc} is current in DC system, P total power consumption in load and V_{dc} the dc voltage:

$$\Delta P_{dc} = 2 \cdot r \cdot l \cdot I_{dc}^2 = 2 \cdot r \cdot l \cdot \frac{P^2}{V_{dc}^2} \quad (14.14)$$

ΔP_{dc} power losses in DC system, r the cable resistance per unit length, V_{dc} the DC voltage and l the cable length.

14.5.2 Transformation and Conversion Losses

There are AC-DC conversion losses and DC-DC conversion losses present at different voltage levels in any multilevel DC system [24]. Main losses are conduction and switching losses. Due to partial distribution of current between IGBT

Table 14.3 Conduction losses parameters of IGBT 2—generation [27]

Parameters	Magnitude
u_{T0}	1.1 V
u_{D0}	0.832 V
r_T	11.0 m Ω
r_D	3.55 m Ω

Table 14.4 Switching losses parameters of IGBT 2—generation [27]

Parameter	Magnitude
a_{0Eon}	0.0794
a_{1Eon}	0.0060
a_{2Eon}	2×10^{-5}
a_{0Eoff}	0.493
a_{1Eoff}	0.0239
a_{2Eoff}	-1×10^{-5}
a_{0Erec}	0.6369
a_{1Erec}	0.029
a_{2Erec}	-6E - 5

and anti-parallel diode, the accurate finding for the conduction losses is becoming difficult. Consideration is made by connecting a series resistance in series to create a voltage drop. According to [25], IGBT module with series resistance exhibits properties very close to an on-state resistance diode, and for this reason, conduction losses can be calculated in a simplified manner.

14.5.3 AC-DC Converter Losses

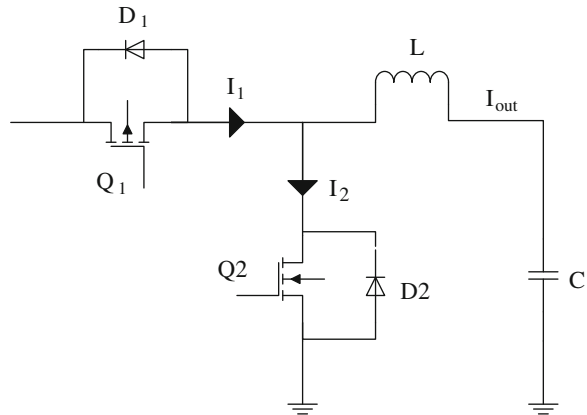
The power electronic converter is a combination of transistor and diode. The power losses in a power electronic converter can be divided into conduction and switching losses [25]. The conduction losses parameters of IGBT 2—generation has been shown in Table 14.3. The average conduction losses in the transistor or diode can be expressed as:

$$\bar{P}_{c.loss,T/D} = u_{T_0/D_0} \left(\frac{1}{2\pi} \pm \frac{\alpha \cos \phi}{8} \right) + r_{T/D} \hat{I}^2 \left(\frac{1}{8} \pm \frac{\alpha \cos \phi}{3\pi} \right) \quad (14.15)$$

where $\bar{P}_{c.loss,T/D}$ the average conduction losses for transistor or diode, u_{T_0} , the threshold voltage of transistor, u_{D_0} threshold voltage of diode, r_T , differential resistance of transistor, r_D differential resistance of diode.

The switching losses in the power electronic converters occur during the turn on and turn off the power semiconductor and depend on the current blocking voltage, the chip temperature and the current which are represented in characteristic maps

Fig. 14.7 Basic topology of buck converter



of the energy losses per switch delivered by the manufacturer [26]. The switching losses parameters of IGBT 2—Generation is shown in Table 14.4. The power losses in switching are calculated by the following equation [27].

$$\bar{P}_s = f_s \left[\begin{aligned} & \frac{1}{2\pi} \int_0^{2\pi} E_{onT}(i_T) d\phi + \frac{1}{2\pi} \int_0^{2\pi} E_{offT}(i_T) d\phi \\ & + \frac{1}{2\pi} \int_0^{2\pi} E_{rec}(i_D) d\phi \end{aligned} \right] \frac{U_{dc}}{U_{dcref}} \quad (14.16)$$

where E_{onT} , the switching on losses of the transistor, E_{offT} the switching off losses of the transistor, and E_{rec} , the switching off losses of the diode.

14.5.4 DC-DC Converter

The power losses in a power electronic DC-DC converter can be divided into conduction and switching losses, where conduction losses consist of inductor conduction losses and MOSFET conduction losses [28] (Fig.14.7).

- Inductor Conduction Losses

Inductor conduction losses is as follows

$$P_L = I_L^2 \times R_L \quad (14.17)$$

where R_L is the DC-Resistance of the inductor,

The inductor rms current (I_L):

$$I_L = I_o^2 + \frac{\Delta I^2}{12} \quad (14.18)$$

where I_o the output current and ΔI the ripple current.

Typically, ΔI is about 30 % of the output current. Therefore, the inductor current can be calculated as:

$$I_L = I_o \times 1.00375 \quad (14.19)$$

Because the ripple current contributes only 0.375 % of I_L , it can be neglected. The power dissipated in the inductor now can be calculated as:

$$P_L = I_o^2 \times R_L \quad (14.20)$$

- Power Dissipated in the MOSFETs

The power dissipated in the high-side MOSFET is given by:

$$P_{Q1} = I_{rms_Q1}^2 \times R_{DSON1} \quad (14.21)$$

where R_{DSON1} is the on-time drain-to-source resistance of the high-side MOSFET.

$$P_{Q1} = \frac{V_o}{V_{IN}} \left(I_o^2 + \frac{\Delta I^2}{12} \right) R_{DSON1} \quad (14.22)$$

The power dissipated in the low-side MOSFET is given by:

$$P_{Q2} = I_{rms_Q2}^2 \times R_{DSON2} \quad (14.23)$$

where R_{DSON2} is the on-time drain-to-source resistance of the low-side MOSFET.

$$P_{Q2} = \left(1 - \frac{V_o}{V_{IN}} \right) \left(I_o^2 + \frac{\Delta I^2}{12} \right) R_{DSON2} \quad (14.24)$$

The total power dissipated in both MOSFET's is given by:

$$P_{FET} = P_{Q1} + P_{Q2} \quad (14.25)$$

$$P_{FET} = \left(I_o^2 + \frac{\Delta I^2}{12} \right) \left[\left(1 - \frac{V_o}{V_{IN}} \right) R_{SDON2} + \frac{V_o}{V_{IN}} R_{SDON1} \right] \quad (14.26)$$

where

$$\Delta I = \frac{(V_{IN} \times V_o - V_o^2)}{L \times f \times V_{IN}} \quad (14.27)$$

and:

L = Inductance (H)

f = Frequency (Hz)

Fig. 14.8 Cable size versus prices in Indian scenario

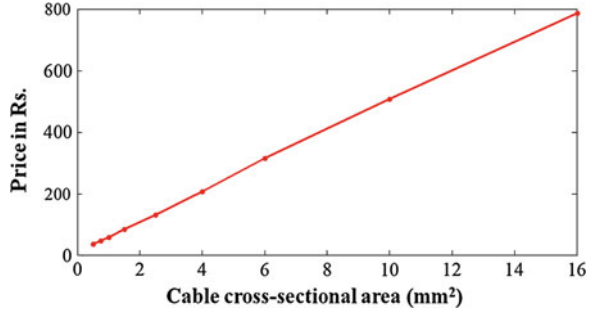


Table 14.5 Investigated appliances, appliance ratings and estimated on time per day

Product name	Quantity	Ratings			Appliance on time in a day
		Power rating (W)	Current rating (A)	Voltage Rating (V)	
Light bulb LED	4	7	0.60	12 DC	10
Light bulb CFL	2	12	1.00	12 DC	10
Microwave oven	1	235	10.00	24 DC	1
Induction stove	1	2000	10.00	230 AC	2
Electric geyser	1	1500	8.00	230 AC	1
Sandwich maker	1	550	23.00	24 DC	0.5
Coffee maker	1	135	11.00	12 DC	0.5
Refrigerator (DC)	1	72	3.00	24 DC	12
Water purifier	1	11	0.50	24 DC	1
Ventilation fan	4	20	0.90	24 DC	5
Submersible pump	1	240	10.00	24 DC	0.5
Washing machine	1	70	3.00	24 DC	0.5
Vacuum cleaner	1	95	8.00	12 DC	0.25
Window unit AC	2	800	33.30	24 DC	12
Laptop	1	65	3.34	19.5 DC	7
Perdonal computer	1	170	14.00	12 DC	5
External modem	1	5	0.43	12 DC	24
15.6"LCD television	1	30	2.50	12 DC	5
Ceiling fan	4	20	1.70	12 DC	4
Hair dryer	1	425	15.00	24 DC	0.5
Cell phone	4	4	0.30	12 DC	5
Hybrid car	1	3000	12.50	240 DC	10

V_{IN} = Input voltage (V)

V_o = Output voltage (V)

- MOSFET Conduction Losses

Table 14.6 Cable size, power loss and energy consumption for DC system

Product Name	Cable Size (mm ²)	Cable length (meter)	Energy Loss in feeder (kWh/yr)	Total Energy Consumption (kWh/yr)
Light Bulb LED	4	40	0.23	102.43
Light Bulb CFL	4	30	0.47	88.07
Microwave oven	6	10	1.05	86.82
Induction Stove	1.5	20	16.74	1476.74
Electric Geyser	1.5	30	8.04	555.54
Sandwich Maker	35	20	0.95	101.32
Coffee Maker	25	20	0.30	24.94
Refrigerator DC	4	20	3.39	318.75
Water Purifier	1.5	20	0.02	4.04
Ventilation fan	1.5	30	0.51	146.51
Submersible Pump	6	10	0.52	44.32
Washing Machine	6	25	0.12	12.89
Vacuum Cleaner	16	15	0.09	8.76
Window Unit AC	25	10	33.42	7041.42
Laptop	10	40	1.96	168.04
Personal Computer	25	15	3.69	313.94
External Modem	1.5	30	0.56	44.36
15.6" LCD Television	6	20	0.65	55.40
Ceiling Fan	4	20	0.36	117.16
Hair Dryan	16	15	0.66	78.22
Cell Phone	1.5	20	0.04	29.24
Hybrid Car	1.5	10	65.40	11015.40
Total Energy in kWh/year			139.17	21834.31

For typical buck power supply designs, the inductor's ripple current, ΔI , is less than 30 % of the total output current, so the contribution of $\Delta I/12$ to the is negligible and can be dropped to get:

$$P_{FET} = I_o^2 \left[\frac{V_o}{V_{IN}} (R_{SDON1} - R_{SDON2}) + R_{SDON2} \right] \quad (14.28)$$

Note that when $R_{SDON1} = R_{SDON2}$, then:

$$P_{FET} = I_o^2 \times R_{SDON2} \quad (14.29)$$

The power dissipated in the MOSFET is independent of the output voltage. By using Eq. (14.29) the conduction losses of MOSFET can be calculated at any output voltage. On the other side, inductor conduction losses and switching losses etc. are independent of output voltage and remains constant with change in output voltage [22].

Hence, P_D now can be computed as:

$$P_D = P_L + P_{FET} + \text{other losses} \quad (14.30)$$

There are some other types of losses such as the MOSFET switching losses, quiescent current etc. At any output voltage, the overall efficiency can be calculated by the known total power supply losses and power supply output power.

$$\eta = \frac{P_o}{P_o + P_D} \quad (14.31)$$

14.6 Total Cable Cost

The voltage drop across the feeder cable and current is high for the 12 V DC systems. The dependency of these losses is on the household appliances as well as on the cable size (length and cross sectional area). For the 12 V DC systems, the current is double for the appliances of same power rating compared to the 24 V DC systems. Hence, power losses and voltage drops will decrease by increasing the voltage rating. If the wire resistance is reduced then the power losses across the cable can be reduced, as the resistance is inversely proportional to the cross section of the wire. The losses in the cable can be reduced by increasing its cross-sectional area. For example in a load of 500 W the power losses reduces 40 % if a 2.5 mm² cable is used instead of a 1.5 mm² cable. However, when the cross-sectional area increases it will definitely increase the copper cost used in the cable. The total cost of the cable can be minimized by minimizing the cross sectional area of the cable [29].

The total cost of the cable is calculated as the sum of the investment cost of the cable and the cost of the losses in the cable.

The total annual cost is calculated as:

$$C_t = C_c + \frac{W_{fl}}{\text{year}} \times N \times C_e \quad (14.32)$$

where C_t the total cost, C_c the cable cost, W_{fl} feeder energy loss, N life time and C_e energy cost. The life time is assumed to be 25 years and the energy cost Rs.1 / kWh. From Fig. 14.8, it is seen that the copper wire cost increases almost linearly with the cross section of wire.

The annual cable cost can be expressed as:

$$C_c = (C_1 + C_2A)\text{Rs.} \quad (14.33)$$

The annual cost of energy waste can be calculated as:

$$C_{ew} = \frac{C_3}{A}\text{Rs.} \quad (14.34)$$

Total annual cost

$$C_t = \left(C_1 + C_2 A + \frac{C_3}{A} \right) l \quad (14.35)$$

where C_1 , C_2 , C_3 are constant and A is the cross sectional area of conductor.

$$\begin{aligned} C_1 &= 2.662 \text{ Rs./m}, & C_2 &= 1.959 \text{ Rs./mm}^2 \cdot \text{m}, \text{ and} \\ C_3 &= P_r \cdot N \cdot \rho \cdot E_{ON} \cdot \frac{I_{on}}{V_{dc}} \text{ Rs. mm}^2/\text{m} \end{aligned} \quad (14.36)$$

The optimum area that minimizes the total cost can be calculated as

$$\frac{dC_t}{dA} = C_2 - \frac{C_3}{A^2} = 0 \quad (14.37)$$

$$A = \sqrt{\frac{3.75N\rho E_{on}I_{on}}{1.959V_{dc}}} \quad (14.38)$$

The on time in a typical day of different ratings appliances in a building is shown in Table 14.5.

The description of cable size (area of cross section and length) to connect particular appliances to the supply is based on Table 14.6. The energy losses in the feeder and the total energy consumption in each appliances of building for a year is also shown.

14.7 Conclusions

In this chapter, DC grids and Hybrid Electric Vehical (HEV) architechture has been discussed. Topologies and wiring system discussed here are very helpful to understand the most efficient way of interconnection. Tabular data of energy dissipated in DC appliances and the cable cost data representing a easy way to understand the correlation of different parameters associated with losses. Graphical relation of cable cost vs. cable cross-sectional area representing a recent study of indian power economics. The relation is almost linear in nature with some exceptions. So the cost calculation can be done by standard formulation. Overall chapter giving a brief knowledge about DC grid topologies, losses and cost optimization, which are the main requirements to design a DC system.

Acknowledgments This work was supported by the Department of Science and Technology, Government of India, under the Science and Engineering Research Board Fast Track Scheme for Young Scientists (SERC/ET-0123/2012).

References

1. Uhlmann E (1975) Power transmission by direct current. Springer, Berlin, 289
2. International Energy Agency, World Energy Outlook (2011) Paris, France IEA publications
3. Garbesi K, Vossos V, Shen H (2012) Catalog of dc appliances and power system. http://efficiency.lbl.gov/sites/all/files/catalog_of_dc_appliances_and_power_systems_lbnl-5364e.pdf
4. Chiu HJ, Huang HM, Lin LW, and Tseng MH (2005) A multiple input DC-DC converter for renewable energy systems. In: Proceedings of 2005 IEEE international conference on industrial technology, pp 1304–1308
5. Khanna M, Rao ND (2009) Supply and demand of electricity in the developing world. *Annu Rev Resource Econ* 1:567–596
6. Noroozian R, Abedi M, Gharehpetian GB, Hosseini SH (2010) Distributed resources and DC distribution system combination for high power quality. *Int J Electr Power Energy Syst* 32(7):769–781
7. Solero L, Lidozzi A, Pomilio JA (2005) Design of multiple-input power converter to hybrid vehicles. *IEEE Trans Power Electron* 20(5):1007–1016
8. Jiang W, Zhang Y (2011) Load sharing techniques in hybrid power systems for dc microgrids. In: Proceedings of 2011 IEEE power and energy engineering conference, pp 1–4
9. Ahmad Khan N (2012). Power loss modeling of isolated AC–DC converter. Dissertation, KTH
10. Hayashi Y, Takao K et al (2009) Fundamental study of high density DC/DC converter design based on sensitivity analysis. In: IEEE telecommunications energy conference (INTELEC), pp 1–5
11. Kang T, Kim C et al (2012) A design and control of bi-directional non-isolated DC-DC converter for rapid electric vehicle charging system. In: Twenty-seventh IEEE annual applied power electronics conference and exposition (APEC), pp 14–21
12. Sizikov G, Kolodny A et al (2010) Efficiency optimization of integrated DC-DC buck converters. In: 17th IEEE international conference on electronics circuits and systems (ICECS), pp 1208–121
13. Vorperian V (2010) Simple efficiency formula for regulated DC-to-DC converters. *IEEE trans Aerosp Electron* 46(4):2123–2131
14. Wens M, Steyaert M (2011) Basic DC-DC converter theory. Design and implementation of fully-integrated inductive DC-DC converters in standard CMOS, Springer
15. Zhang F, Du L et al. (2006) A new design method for high efficiency DC-DC converters with flying capacitor technology. In: IEEE twenty-first annual applied power electronics conference and exposition (APEC), pp 92–96
16. Starke M, Tolbert L M, Ozpineci B (2008) AC vs. DC distribution: a loss comparison. In proceedings. of transmission and distribution conference and exposition, pp 1–7
17. Savage P, Nordhaus R et al (2010) DC microgrids: benefits and barriers. published for Renewable Energy and International Law (REIL) project. Yale School of Forestry and Environmental Studies, pp 0–9
18. Pellis J, P J I et al (1997). The DC low-voltage house. Dissertation, Netherlands Energy Research Foundation ECN
19. Chauhan R K, Rajpurohit B S, Pindoriya N M (2012) DC power distribution system for rural applications. In: Proceedings of 8th national conference on indian energy sector, pp 108–112
20. Salonen P, Kaipia T, Nuutinen P, Peltoniemi P, Partanen J (2008) An LVDC distribution system concept. Nordic Workshop on Power and Industrial Electronics. A3-1–A3-16
21. Hossain MJ, Pota HR, Ugrinovskii V, Ramos RA (2009) Robust STATCOM control for the enhancement of fault ride-through capability of fixed speed wind generators. *IEEE Control Applications (CCA) and Intelligent Control (ISIC)*, pp.1505–1510
22. Dastgeer F, Kalam A (2009) Efficiency comparison of DC and AC distribution systems for distributed generation. In: IEEE power engineering conference, pp 1–5

23. Nilsson D, Sannino A (2004) Efficiency analysis of low-and medium-voltage dc distribution systems. In: IEEE power engineering society general meeting, pp 2315–2321
24. Peterson A Lundberg S (2002) Energy efficiency comparison of electrical systems for wind turbines, Nordic workshop on power and industrial electronics (NORPIE)
25. Schroeder D(2008) Leistungselektronische Schaltungen (Power Electronic Circuits), Springer, Berlin
26. Muehlbauer K, Gerling D (2012) Experimental verification of energy efficiency enhancement in power electronics at partial load. In: 38th annual conference on IEEE industrial electronics society (IECON), pp.394–397. doi: [10.1109/IECON.2012.6388788](https://doi.org/10.1109/IECON.2012.6388788)
27. Muehlbauer K, Bachl F, Gerling D (2011) Comparison of measurement and calculation of power losses in AC/DC-converter for electric vehicle drive. In: International conference on electrical machines and systems (ICEMS), pp 1–4
28. Raj A (2010) PMP-DCDC controllers calculating efficiency: application report. <http://www.ti.com/lit/an/slva390/slva390.pdf>. Accessed February 2010
29. Amin M, Arafat Y et al. (2011) Low voltage DC distribution system compared with 230 V AC. In: IEEE electrical power and energy conference (EPEC), pp 340–345